First-principles study of ground- and excited-state properties of MgO, ZnO, and CdO polymorphs

A. Schleife, F. Fuchs, J. Furthmüller, and F. Bechstedt

Institut für Festkörpertheorie und -optik, Friedrich-Schiller-Universität, Max-Wien-Platz 1, 07743 Jena, Germany

An *ab initio* pseudopotential method based on density functional theory, generalized gradient corrections to exchange and correlation, and projector-augmented waves is used to investigate structural, energetical, electronic, and optical properties of MgO, ZnO, and CdO in rocksalt, cesium chloride, zinc blende, and wurtzite structure. In the case of MgO we also examine the nickel arsenide structure and a graphitic phase. The stability of the ground-state phases rocksalt (MgO, CdO) and wurtzite (ZnO) against hydrostatic pressure and biaxial strain is studied. We also present the band structures of all polymorphs as well as the accompanying dielectric functions. We discuss the physical reasons for the anomalous chemical trend of the ground-state geometry and the fundamental gap with the size of the group-II cation in the oxide. The role of the shallow Zn3d and Cd4d electrons is critically examined.

I. INTRODUCTION

Currently the optical properties of wide band-gap semiconductors such as zinc oxide (ZnO) are of tremendously increasing interest, in response to the industrial demand for optoelectronic devices operating in the deep blue or ultraviolet spectral region. Under ambient conditions ZnO is crystallizing in wurtzite (*w*) structure. Its tendency to be grown as fairly high residual *n*-type material illustrates the difficulty to achieve its *p*-type doping. Nevertheless, the potential of ZnO for optoelectronics[1] but also for spintronics[2] (e.g., in combination with MnO) renders it among the most fascinating semiconductors now and of the near future.

Heterostructures with other materials are most important for optoelectronic applications.[3,4] One important class of crystals for heterostructures with ZnO could be the other group-II oxides and alloys with these compounds. Another IIB oxide is CdO which however has a much smaller fundamental energy gap.[5] On the other hand, the group-IIA oxide with the smallest cation, MgO, possesses a much larger energy gap.[6] Consequently, combinations of these oxides with ZnO should lead to type-I heterostructures with ZnO (CdO) as the well material and MgO (ZnO) as the barrier material. However, there are at least two problems for the preparation of heterostructures: (i) The group-II oxides MgO, ZnO, and CdO in their ground states do not represent an isostructural series of compounds with a common anion, which means the ground states are given by different crystal structures: the cubic rocksalt (MgO, CdO) or the hexagonal wurtzite (ZnO) one.[5] (ii) The in-plane lattice constants of two oxides grown along the cubic [111] or hexagonal [0001] direction are not matched.

Among several other properties of the group-II oxides that are not well understood is their behavior under hydrostatic and biaxial strain as well as their stability: Which are possible high-pressure phases? Are there any strain-induced phase transitions? Which role do the *d*-electrons play for ZnO and CdO? Other open questions concern the influence of the atomic geometry on the band structure and, hence, on the accompanying optical properties. Furthermore, the band-gap anomaly of CdO has to be clarified: While the band gaps of the common-cation systems CdTe, CdSe, CdS, and CdO show an increase of the fundamental gap along the decreasing anion size until CdS, the value for CdO is smaller than that of CdS.[7] A similar anomaly occurs along the row ZnTe, ZnSe, ZnS, and ZnO,[7] however, the gap variation is much smaller. Such gap anomalies are also observed for III-V semiconductors with a common cation: one example is the row InSb, InAs, InP, and InN,[8] where the anomaly for InN has been traced back to the extreme energetical lowering of the N2s orbital with respect to the Sb5s, As4s, and P3s levels and the small band-gap deformation potential of InN.[8]

In this paper, we report well-converged *ab initio* calculations of the ground- and excited-state properties of the most important polymorphs of the group-II oxides MgO, ZnO, and CdO. In Sec. II the computational methods are described. Atomic geometries and the energetics are presented in Sec. III for cubic and hexagonal crystal structures. In Sec. IV we discuss the corresponding band structures and the electronic dielectric functions. Finally, a brief summary and conclusions are given in Sec. V.

II. COMPUTATIONAL METHODS

Our calculations are based on the density functional theory (DFT)[9] in local density approximation (LDA) with generalized gradient corrections (GGA)[10] according to Perdew and Wang (PW91).[11] The electron-ion interaction is described by pseudopotentials generated within the projector-augmented wave (PAW) scheme[12–14] as implemented in the Vienna Ab initio Simulation Package (VASP).[15] The PAW method allows for the accurate treatment of the first-row element oxygen as well as the Zn3d and Cd4d electrons at relatively small plane wave cutoffs.

For the expansion of the electronic wave functions we use plane waves up to kinetic energies of 29.4 Ry (MgO in wurtzite, rocksalt, CsCl, NiAs, and graphitic-like structure, ZnO in zinc blende and wurtzite structure, and CdO in rocksalt and wurtzite structure) and 33.1 Ry (MgO in zinc-blende structure, ZnO in CsCl and rocksalt structure, and CdO in

CsCl and zinc-blende structure), respectively. To obtain converged results for the external pressures (trace of the stress tensor) we increased the plane wave energy-cutoff to 51.5 Ry uniformly for all materials. The Brillouin-zone (BZ) integrations in the electron density and the total energy are replaced by summations over special points of the Monkhorst-Pack type.[16] We use $8 \times 8 \times 8$ meshes for cubic systems and $12 \times 12 \times 7$ for hexagonal polymorphs.

A first approach to qualitatively reliable band structures is using the eigenvalues of the Kohn-Sham (KS) equation.[10] They also allow the computation of the electronic density of states (DOS). We apply the tetrahedron method[17] to perform the corresponding BZ integration with **k**-space meshes $20 \times 20 \times 20$ for cubic crystals or $30 \times 30 \times 18$ for hexagonal structures. For the cubic polymorphs the frequency-dependent complex dielectric function $\varepsilon(\omega)$ is a scalar, but it possesses two independent tensor components $\varepsilon_{xx}(\omega) = \varepsilon_{yy}(\omega)$ and $\varepsilon_{zz}(\omega)$ in the cases of hexagonal systems. In independent-particle approximation it can be calculated from the Ehrenreich-Cohen formula.[18] For the BZ integration in this formula we use refined **k**-point meshes of $50 \times 50 \times 31$ for hexagonal structures and $40 \times 40 \times 40$ for cubic crystals. In particular, the frequency region below the first absorption peak in the imaginary part depends sensitively on the number and distribution of the **k** points. The resulting spectra have been lifetime-broadened by 0.15 eV but are converged with respect to the used **k**-point meshes.

III. GROUND-STATE PROPERTIES

A. Equilibrium phases

For the three oxides under consideration, MgO, ZnO, and CdO we study three cubic polymorphs: the B1 rocksalt (rs or NaCl) structure with space group $Fm3m$ (O_h^5), the B3 zinc-blende (zb or ZnS) structure with space group $F\bar{4}3m$ (T_d^2) and the B2 CsCl structure with $Pm3m$ (O_h^1). In the case of the hexagonal crystal system we focus our attention on the B4 wurtzite (w) structure with space group $P6_3mc(C_{6v}^4)$ but we also investigate the B8$_1$ NiAs structure with $P6_3/mmc$ (D_{6h}^4) symmetry and a graphitic-like structure with the same space group[19] for MgO, which we call h-MgO, according to Ref. 20. The fourfold-coordinated w and zb structures are polytypes with the same local tetrahedral bonding geometry, but they differ with respect to the arrangement of the bonding tetrahedrons in [0001] or [111] direction. Their high-pressure phases could be the sixfold-coordinated NaCl or eightfold-coordinated CsCl structures. In the cubic zb and rs phases the cation and anion sublattices are displaced against each other by different distances parallel to a body diagonal, $(1,1,1)a_0/4$ for zb and $(1,1,1)a_0/2$ for rs, respectively. There are also several similarities for the three hexagonal phases wurtzite, NiAs, and h-MgO. In the NiAs structure the sites of two ions are not equivalent. For the ideal ratio $c/a = \sqrt{8/3}$ of the lattice constants the anions (As) establish a hexagonal close-packed (hcp) structure, whereas the cations (Ni) form a simple hexagonal (sh) structure. Each cation has four nearest anion neighbors, whereas each anion has six nearest neighbors, four cations, and two

anions. The latter ones form linear chains parallel to the c axis. In the case of h-MgO the cations and anions form a graphitic-like structure[21] with B_k BN symmetry, in comparison wurtzite leads to flat bilayers because of a larger u parameter and an additional layer-parallel mirror plane. Furthermore the lattice constant c is only somewhat larger than the in-plane nearest neighbor distance, so that h-MgO is essentially fivefold coordinated.

To determine the equilibrium lattice parameters the total energy was calculated for different cell volumes, while the cell-shape and internal parameters were allowed to relax. Using the Murnaghan equation of state (EOS)[22] we obtained the energy-volume dependences $E=E(V)$, the corresponding fits are represented in Fig. 1. For the polymorphs of MgO, ZnO, and CdO being most stable in certain volume ranges around the equilibrium volumes, these fits lead to the equilibrium values for the volume V_0 and the total energy E_0 per cation-anion pair, as well as the isothermal bulk modulus B, and its pressure coefficient $B'=(dB/dp)_{p=0}$. The binding energy E_B has been calculated as the corresponding total energy E_0 at zero temperature reduced by atomic total energies computed with spin polarization. In Table I these parameters are summarized together with the lattice parameters we obtained.

The $E(V)$ curves in Fig. 1 clearly show that under ambient conditions the group-II oxides crystallize either in rs (MgO and CdO) or w (ZnO) structure. However, the binding energies of the atoms in rs and w structure are rather similar, especially for CdO. The energy gains due to electrostatic attraction on smaller distances (NaCl) and due to the better overlap of sp^3 hybrids (wurtzite) result in a sensitive energy balance. Therefore we cannot give a simple explanation why one of these crystal structures has to be favored over the other one. Furthermore we observe an anomalous structural trend along the cation row Mg, Zn, and Cd, which follows the anomalous trend of their covalent radii 1.36, 1.25, and 1.48 Å.[36] Together with the oxygen radius of 0.73 Å the resulting nearest-neighbor distances 2.09, 1.98, and 2.21 Å in the tetrahedrally coordinated wurtzite structure take a minimum for ZnO. That means besides the strong covalent bonds due to sp^3 hybrid overlapping, also significant energy gain due to the Madelung energy occurs. As a result of the *ab initio* calculations (cf. Table I) the nearest-neighbor distances in the sixfold-coordinated rocksalt structure show a minor monotonous variation 2.13, 2.17, and 2.39 Å. Also the corresponding ionic energies, the repulsive interaction, and the Madelung energy follow a monotonous trend. The sequence of the ratios of the nearest-neighbor distances of these two polymorphs with about 0.98, 0.91, and 0.93 may also be considered as an indication why ZnO exhibits another equilibrium structure as MgO and CdO and, hence, for the nonexistence of an isostructural series. Both the favorization of w or rs structure, as well as the cationic trend we observed, may be explained with the ideas of Zunger.[37] Within his model he examined over 500 different compounds and predicted the correct equilibrium structures for the three materials we investigated.

Comparing the results with data of recent measurements or other first-principles calculations, we find excellent agreement (cf. Table I). For ZnO the wurtzite ground-state and the
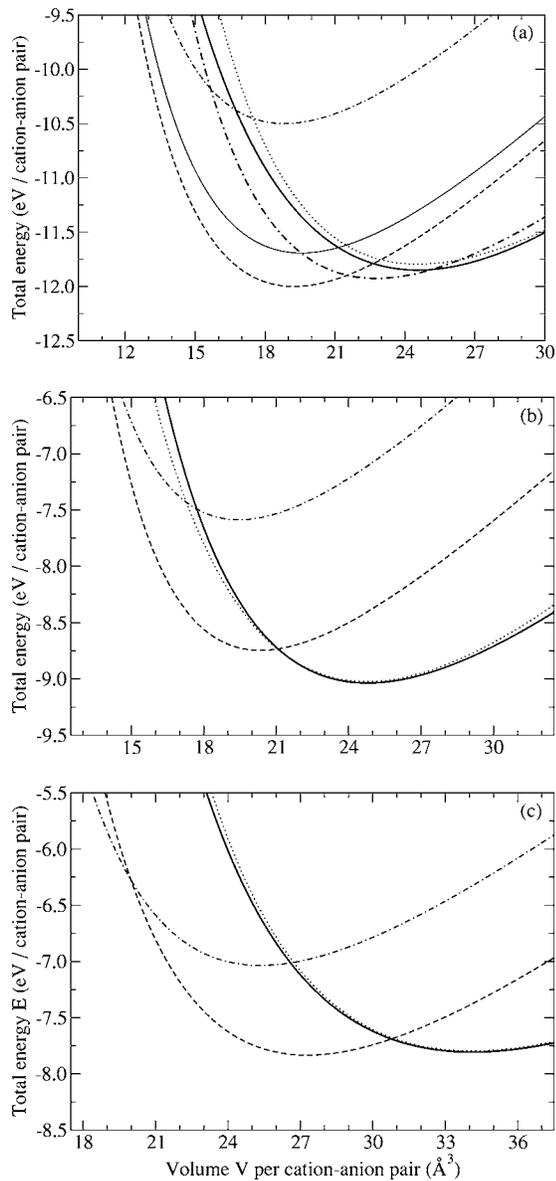
FIG. 1. The normalized total energy versus volume of one cation-oxygen pair. Several polymorphs have been studied for MgO (a), ZnO (b), and CdO (c). *w*: thick solid line, NiAs structure: thin solid line, *h*-MgO structure: long dash-dotted line, rs: dashed line, zb: dotted line, CsCl structure: dash-dotted line.

NaCl (and CsCl) high-pressure phases are confirmed by experimental studies[28,29,33,38,39] and other *ab initio* calculations.[25,28,29,38,39] Experimental results for the rocksalt ground state of MgO[24] and CdO[27] exist, as well as other calculations for the equilibrium structure[25–27,34] and the high-pressure phase (CsCl).[25,34] In the case of CdO also the CsCl structure has been studied experimentally.[40]

Our computed lattice parameters for the CdO polymorphs show excellent agreement, in particular compared with the results of Jaffe *et al.*[25] These authors also use a DFT-GGA scheme but expand the wave functions in localized orbitals of Gaussian form. However, also the agreement with values from other computations is excellent. Most of them use a DFT-LDA scheme which tends to an overbinding effect, i.e.,

too small lattice constants, too large bulk moduli, and too large binding energies. The overestimation of the binding energies of ZnO polymorphs in Ref. 31 is probably a consequence that non-spin-polarized atomic energies have been substracted.

The DFT-GGA scheme we used tends to underestimate slightly the bonding in the considered group-II oxide polymorphs. This underestimation results in an overestimation of the lattice constants of about 1%. In the case of the *c*-lattice constants of *w*-ZnO and the a_0 constant of rs-CdO this discrepancy increases to roughly 2%. Also our calculated bulk moduli are always smaller than the experimental ones, which may be due to the mentioned underestimation. Besides the limitation of the computations we cannot exclude that sample-quality problems play a role for these discrepancies. For rs-MgO, *w*-ZnO, and rs-CdO the computed binding energies are close to the measured ones. The theoretical underestimation only amounts to 1, 5, or 7%, which are small deviations.

B. Pressure- and strain-induced phase transitions

Structural changes in the form of pressure-induced phase transitions are studied in detail in Fig. 2 for ZnO. Usually the Gibbs free energy $G=U+pV-TS$ as the appropriate thermodynamic potential governs the crystal stability for given pressure and temperature. Its study however requires the knowledge of the full phonon spectrum. Therefore, we restrict ourselves to the discussion of the low-temperature limit, more strictly speaking to the electronic contribution to the enthalpy $H=E+pV$ with the internal energy $U(V) \approx E(V)$ and the external pressure obtained as the trace of the stress tensor. The zero-point motional energy is neglected. Such an approach is sufficient for the discussion of the pressure-induced properties of relatively hard materials for temperatures below that given by the maximum frequency of the phonon spectrum.[41] For a given pressure the crystallographic phase with the lowest enthalpy is the most stable one, and a crossing of two curves indicates a pressure-induced first-order phase transition.

From Fig. 2 we derived the equilibrium transition pressure p_t. Using p_t we obtained from p over V plots the initial volume V_i and final volume V_f for the transitions, given here in units of the equilibrium volume V_0 of the wurtzite polymorph. We derive the values $p_t=11.8$ GPa ($V_i=0.92V_0$, $V_f=0.77V_0$) for the transition wurtzite →NaCl and $p_t=261$ GPa ($V_i=0.50V_0$, $V_f=0.47V_0$) for the transition NaCl →CsCl. The first values are in rough agreement with the experimental findings $p_t=9.1$ GPa ($V_t=0.82V_0$),[33] $p_t \approx 10$ GPa,[38] or $p_t \approx 9$ GPa,[42] though our calculations indicate a slightly higher stability of the wurtzite structure over the rocksalt one. The computed p_t value is in reasonable agreement with other calculations (see Ref. 25, and references therein). Another pressure-induced phase transition between NaCl and CsCl structure is found at a transition pressure of 261 GPa, very similar to a previous calculation[25] which predicted a value of $p_t=256$ GPa.

Applying the common-tangent method the $E(V)$ curves in Figs. 1(a) and 1(c) for MgO and CdO already show that

TABLE I. Ground-state properties of equilibrium and high-pressure phases of MgO, ZnO, and CdO. All the experimental binding energies [*]) are taken from Ref. 23 as heat of vaporization or heat of atomization.

Oxide	Phase	Lattice parameter (Å or dimensionless)			B (GPa)	B'	Binding energy (eV/pair)	Reference
MgO	Wurtzite	$a=$	$c=$	$u=$				
		3.322	5.136	0.3916	116.9	2.7	10.02	This work
		3.169	5.175	0.3750	137	$\cdots$	10.85	Theor.[a]
	h-MgO	$a=$	$c=$	$u=$				
		3.523	4.236	0.5002	124.8	4.3	10.09	This work
		3.426	4.112	0.5000	148	$\cdots$	11.09	Theor.[a]
	Rocksalt	$a_0=$						
		4.254			148.6	4.3	10.17	This work
		4.212			$\cdots$	$\cdots$	10.26[*])	Exp.[b]
		4.247			169.1	3.3	10.05	Theor.[c]
		4.197			169.0	4.2	$\cdots$	Theor.[d]
		4.253			150.6	$\cdots$	$\cdots$	Theor.[e]
		4.145			178.0	$\cdots$	11.47	Theor.[a]
	Cesium chloride	$a_0=$						
		2.661			140.3	4.1	8.67	This work
		2.656			152.6	3.4	8.54	Theor.[c]
ZnO	Wurtzite	$a=$	$c=$	$u=$				
		3.283	5.309	0.3786	131.5	4.2	7.20	This work
		3.258	5.220	0.382	181	4	7.52[*])	Exp.[f]
		3.250	5.204	$\cdots$	183	4	$\cdots$	Exp.[g]
		3.238	5.232	0.380	154	4.3	$\cdots$	Theor.[f]
		3.292	5.292	0.3802	133.7	3.8	7.69	Theor.[c]
		3.198	5.167	0.379	159.5	4.5	$\cdots$	Theor.[h]
		3.183	5.124	0.380	162	$\cdots$	10.64	Theor.[i]
	Zinc blende	$a_0=$						
		4.627			131.6	3.3	7.19	This work
		4.633			135.3	3.7	7.68	Theor.[c]
		4.504			160.8	5.7	$\cdots$	Theor.[h]
	Rocksalt	$a_0=$						
		4.334			167.8	5.3	6.91	This work
		4.275			194	4.8	$\cdots$	Exp.[j]
		4.287			218	4	$\cdots$	Exp.[f]
		4.271			228	4	$\cdots$	Exp.[g]
		4.283			202.5	3.5	$\cdots$	Exp.[k]
		4.272			198	4.6	$\cdots$	Theor.[f]
		4.345			172.7	3.7	7.46	Theor.[c]
		4.316			175	5.4	$\cdots$	Theor.[j]
		4.225			209.1	2.7	$\cdots$	Theor.[h]
		4.213			210	$\cdots$	10.43	Theor.[i]
	Cesium chloride	$a_0=$						
		2.690			162.4	4.7	5.76	This work
		2.705			156.9	3.8	6.33	Theor.[c]
CdO	Wurtzite	$a=$	$c=$	$u=$				
		3.678	5.825	0.3849	92.7	4.7	5.97	This work
		3.660	5.856	0.3500	86	4.5	5.30	Theor.[l]
	Zinc blende	$a_0=$						
		5.148			93.9	5.0	5.96	This work

TABLE I. (*Continued.*)

Oxide	Phase	Lattice parameter (Å or dimensionless)	B (GPa)	B'	Binding energy (eV/pair)	Reference
		5.150	82	3.0	5.18	Theor.[l]
	Rocksalt	$a_0=$				
		4.779	130.5	5.0	6.00	This work
		4.696	148	4	6.40*)	Exp.[m]
		4.770	130	4.1	5.30	Theor.[l]

[a]Reference 20.
[b]Reference 24.
[c]Reference 25.
[d]Reference 26.
[e]Reference 27.
[f]Reference 28.
[g]Reference 29.

[h]Reference 30.
[i]Reference 31.
[j]Reference 32.
[k]Reference 33.
[l]Reference 34.
[m]Reference 35.

pressure-induced phase transitions are hardly observable or should occur at high transition pressures (and hence small transition volumes). In the case of MgO the crossing of the enthalpies gives a value of $p_t=508$ GPa for the transition NaCl→CsCl structure. For CdO we obtain $p_t \approx 85$ GPa for the transition NaCl→CsCl structure. In comparison with the result of a previous calculation[27] we find good agreement. Another predicted value amounts to 515 GPa (see Ref. 25, and references therein). Also the CdO value is in excellent agreement with other DFT-GGA calculations $p_t=89$ GPa[35] and even with the result of measurements $p_t=90$ GPa.[40]

For MgO [cf. Fig. 1(a)] we have to mention an interesting result for negative pressures: at large volumes of about $1.3V_0$, indeed wurtzite is more stable than the NaCl structure. However, when we start the atomic relaxation with the wurtzite structure and slightly decrease the cell volume, we observe a transition into the h-MgO structure. The corresponding total energy minimum therefore lies between the rocksalt and the wurtzite minima at a volume of about $V = 1.2V_0$. Around this volume there is no energy barrier between the wurtzite and h-MgO structures and the wurtzite geometry only represents a saddle point on the total energy

FIG. 2. Enthalpy per cation-anion pair of ZnO phases as a function of hydrostatic pressure. w: thick solid line, rs: dashed line, CsCl structure: dash-dotted line. The curve for zinc blende is practically identical with that of wurtzite.

surface, whereas we observe h-MgO to be an intermediate structure on the way from wurtzite to rocksalt, as discussed in Ref. 20. There is another indication for this transition: A decrease of c/a leads to an increase of u, followed by a sudden relaxation into the h-MgO structure.[43] Comparing the u parameters of our wurtzite structures (cf. Table I), we observe that w-MgO has the highest u and so this relaxation is most probable for MgO.

An important point for the above-mentioned heterostructures is the possibility to grow pseudomorphically one material on the other. Because wurtzite ZnO substrates are commercially available, the question arises if such growth of certain polymorphs of MgO or CdO on a w-ZnO substrate with [0001] orientation is possible. For that reason we compare the a-lattice constant of w-ZnO, $a=3.283$ Å, with the corresponding lattice constants a of hexagonal modifications of MgO or CdO and the second-nearest neighbor distances $a_0/\sqrt{2}$ in the cubic cases. The corresponding values are 3.523 (h-MgO), 3.322 (w), and 3.008 Å (rs) for MgO or 3.678 (w), 3.640 (zb), and 3.379 Å (rs) for CdO. With these values the resulting lattice misfits are 7.3, 1.2, and −8.4% for MgO and 12.0, 10.9, and 2.9% for CdO for [0001]/[111] interfaces. From the point of lattice-constant matching pseudomorphic growth of w-MgO and, perhaps, also rs-CdO should be possible on a w-ZnO substrate. This conclusion is confirmed by the total-energy studies (see Fig. 3) for several MgO and CdO polymorphs biaxially strained in [0001] or [111] direction of cation-anion bilayer stacking. For the curves in Fig. 3 we kept the corresponding a-lattice constant fixed at the w-ZnO value and computed the total energy per cation-anion pair for several values of the c-lattice constant of the corresponding hexagonal crystal or of the resulting rhombohedral crystal, the resulting lattice parameters are given in Table II.

The results for MgO are most interesting: In the presence of a weak biaxial strain in [0001] direction of about 1.3% the most energetically favorable geometry is the wurtzite structure with a resulting c-lattice constant of $c=5.21$ Å. The two polymorphs also considered here, the h-MgO structure and the trigonally distorted rs geometry, are much higher in energy. Furthermore the energetical ordering of the MgO poly-
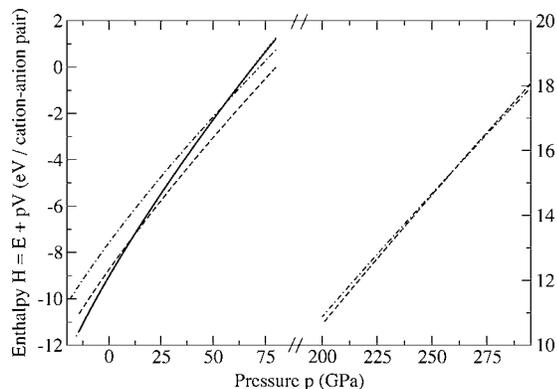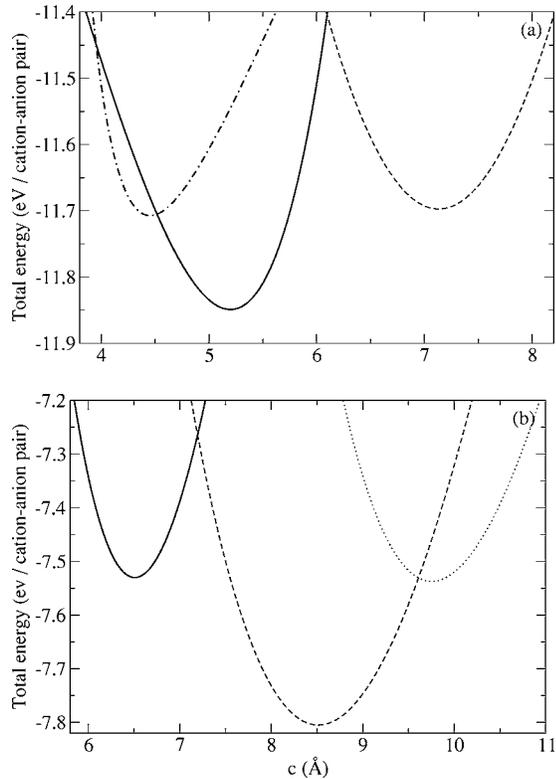
FIG. 3. Total energy of biaxially strained MgO (a) and CdO (b) polymorphs versus the c-lattice constant in [111] or [0001] direction for an a-lattice constant fixed at the value $a=3.283$ Å of wurtzite ZnO. w: thick solid line, rs: dashed line, zb: dotted line, and h-MgO structure: long dash-dotted line.

morphs [cf. Fig. 1(a)] is completely changed and MgO adopts the wurtzite crystal structure of the substrate which is different from its rocksalt geometry in thermal equilibrium. From the u parameters for constrained w-MgO (see Table II) and w-MgO in equilibrium (see Table I) we find that according to Ref. 43 the biaxially strained wurtzite structure should be more stable against a transition into h-MgO, because its u parameter is closer to its ideal value. We conclude that pseudomorphic growth of MgO should be possible on ZnO(0001) substrates. We find a somewhat different situation for CdO. Apart from the large lattice misfit which probably prohibits pseudomorphic growth, its lowest energy structure is still derived from the rs atomic arrangement. Of course, there is a strong trigonal distortion giving rise to a c-lattice constant of $c=8.512$ Å in comparison with the thickness $\sqrt{3}a_0$ of three CdO bilayers in [111] direction at thermal equilibrium with $c=8.277$ Å. In the case of CdO the two other crystallographic structures, w and zb, are energeti-

TABLE II. Lattice parameters of the energetically preferred polymorphs of MgO and CdO under biaxial strain along the bilayer-stacking axis.

	w-MgO			rs-CdO	
a (Å)	c (Å)	u		a (Å)	c (Å)
3.283	5.201	0.3856		4.643	8.512

cally less favorable also in the biaxially strained case.

IV. EXCITED-STATE PROPERTIES

A. Band structures and electronic densities of states

To study the influence of the atomic geometry, more precisely the polymorph of the group-II oxide compound, we show in Figs. 4–6 the band structures as calculated within DFT-GGA for the most stable polymorphs in a certain volume range around the equilibrium volume (cf. Sec. III). These are the rocksalt and cesium chloride structures, supplemented by the wurtzite structure and the zinc-blende structure.

By examining the electronic structure in the KS approach one neglects the excitation aspect[44,45] and, hence, underestimates the resulting energy gaps and interband transition energies. In GW approximation the corresponding quasiparticle (QP) energy corrections due to the exchange-correlation self-energy[44–46] amount to about 2.0 eV for ZnO[47] and 3.6 eV for MgO.[48] Nevertheless the independent-particle approximation[49] is frequently a good starting point for the description of optical properties.

For MgO the band structures and densities of states in Fig. 4 indicate an insulator or wide-gap semiconductor independent of the polymorph. Except for the CsCl structure, which has an indirect gap between M and Γ, they all have direct fundamental gaps at the Γ point in the BZ. We find rather similar values 4.5 eV (rs), 3.5 eV (zb), 4.2 eV (NiAs), and 3.3 eV (h-MgO) for the gaps of cubic and hexagonal crystals despite the different lattice constants, coordination, and bonding. There are also similarities in the atomic origin of the bands. The $O2s$ states give rise to weakly dispersive bands 15–18 eV below the valence-band maximum (VBM). They are separated by an ionic gap of 10–12 eV from the uppermost valence bands with band widths below 5 eV. Due to the high ionicity of the bonds the corresponding eigenstates predominately possess $O2p$ character. For the same reason the lowest conduction bands can be traced back to Mg3s states. Also mentionable is the relatively weak dispersion of the uppermost valence bands for the wurtzite and zinc-blende structures which leads, compared with the rocksalt and CsCl structures, to a quite high DOS near the VBM.

For the equilibrium rocksalt polymorph we calculate besides the direct gap at Γ other direct gaps at X and L in the BZ: $E_g(X)=10.43$ eV and $E_g(L)=8.37$ eV. These values are in good agreement with results of other DFT calculations using an LDA exchange-correlation functional and a smaller lattice constant.[48,50,51] In their works,[48,50] these authors computed QP gap openings of about 3.59/2.5 eV (Γ), 3.96/2.5 eV (X), and 4.00/2.5 eV (L) in rough agreement with the values 3.06 eV of Shirley[51] and 2.94 eV derived from the simple Bechstedt–Del Sole formula for tetrahedrally bonded crystals.[52] With these values one obtains QP gaps which approach the experimental values of $E_g(\Gamma)$ $=7.7$ eV, $E_g(X)=13.3$ eV, and $E_g(L)=10.8$ eV[6] or $E_g(\Gamma)$ $=7.83$ eV.[53] A more sophisticated QP value for the fundamental gap is $E_g(\Gamma)=7.79$ eV.[54]

The electronic structures of ZnO plotted in Fig. 5 show several similarities to those of MgO. However, the $O2s$
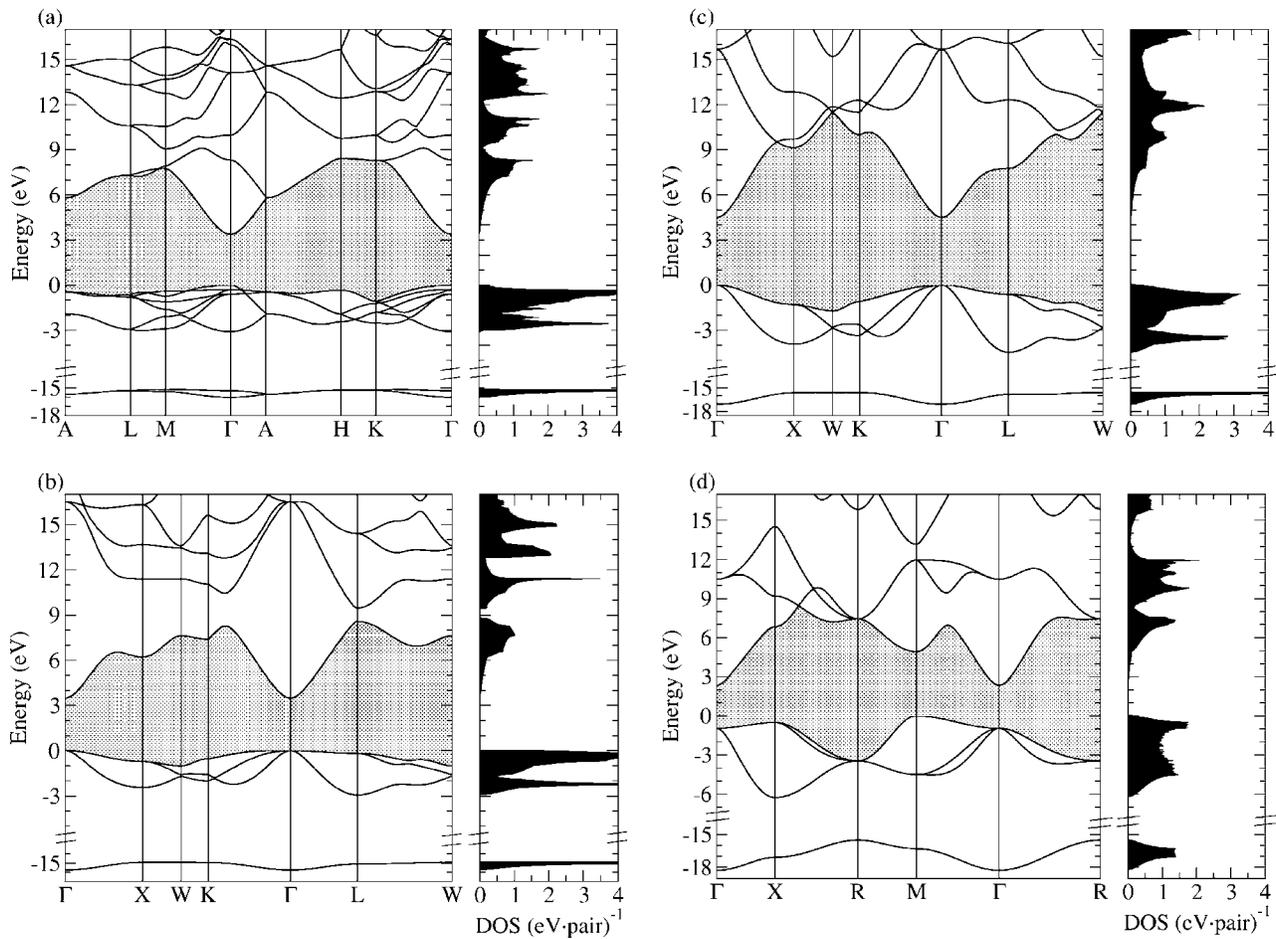
FIG. 4. Band structure and density of states (normalized per pair) for MgO polymorphs calculated within the DFT-GGA framework: (a) wurtzite, (b) zinc blende, (c) rocksalt, and (d) cesium chloride. The shaded region indicates the fundamental gap. The valence band maximum is chosen as energy zero.

bands now appear at about 15.5–18.5 eV below the VBM, and the uppermost valence bands of predominantly $O2p$ character are found in the range from 0 to −4 eV. The lowest conduction-band states (at least near Γ) are dominated by Zn4s states. In comparison with the fundamental energy gaps of MgO those of ZnO are smaller. We compute 0.73 eV (w), 0.64 eV (zb), 1.97 eV (rs) for the direct gap at Γ. However, for the rocksalt geometry the VBM occurs at the L point and therefore this high-pressure phase is an indirect semiconductor with a gap of $E_g(\Gamma-L)=0.75$ eV. This observation is in agreement with findings by room-temperature absorption measurements and DFT-LDA calculations.[25,47,55] Another local valence band maximum which is almost as high as the one at L occurs at the Σ line between K and Γ.

New features that are not observable for MgO are caused by the Zn3d states. These shallow core states give rise to two groups of bands (at Γ) clearly visible in the energy range of 4–6 eV below the VBM, which generally show a splitting and a wave-vector dispersion outside Γ. The huge peaks caused by these basically Zn3d-derived bands are clearly visible in the DOS. Furthermore, the Zn3d states act more subtle on the band structure via the repulsion of p and d bands caused by the hybridization of the respective states. The effects of this pd repulsion can be discussed most easily

for the Γ point in the BZ: In the case of the zb polymorph (with tetrahedral coordination and T_d^2 symmetry), the hybridized anion $p(t_2)$ and cation $d(t_2)$ levels give rise to the three-fold degenerate $\Gamma_{15}(pd)$ and $\Gamma_{15}(dp)$ levels.[56] In the case of wurtzite the levels are doubled at Γ (with respect to the zb-polymorph) due to the band folding along the [111]/[0001] direction. In addition, these states are influenced by a crystal-field splitting. Moreover, in the case of the tetrahedrally coordinated zb and w polymorphs the pd repulsion reduces the fundamental direct gaps at Γ as the $\Gamma_{15}(pd)$ are pushed to higher energies, while the Γ_{1c} conduction band minimum (CBM) remains unaffected. In the case of the rs polymorph (with sixfold coordination and octahedral O_h^5 symmetry), the anion $p(t_1)$ level gives rise to the threefold degenerate $\Gamma_{15}(p)$ valence band, while the symmetry-adapted e (twofold degenerate) and t_2 (threefold degenerate) combination of the cation d states generates the $\Gamma_{12}(d)$ and $\Gamma_{25'}(d)$ bands. The respective states do not hybridize and the pd repulsion as well as the corresponding gap shrinkage vanishes.[56] However in other regions of the BZ, the bands are subject to the pd repulsion and thereby raised at points away from Γ. Consequently the pd repulsion, or more exactly its symmetry forbiddance at Γ, is the reason why the rs polymorph is an indirect semiconductor. Compared to InN
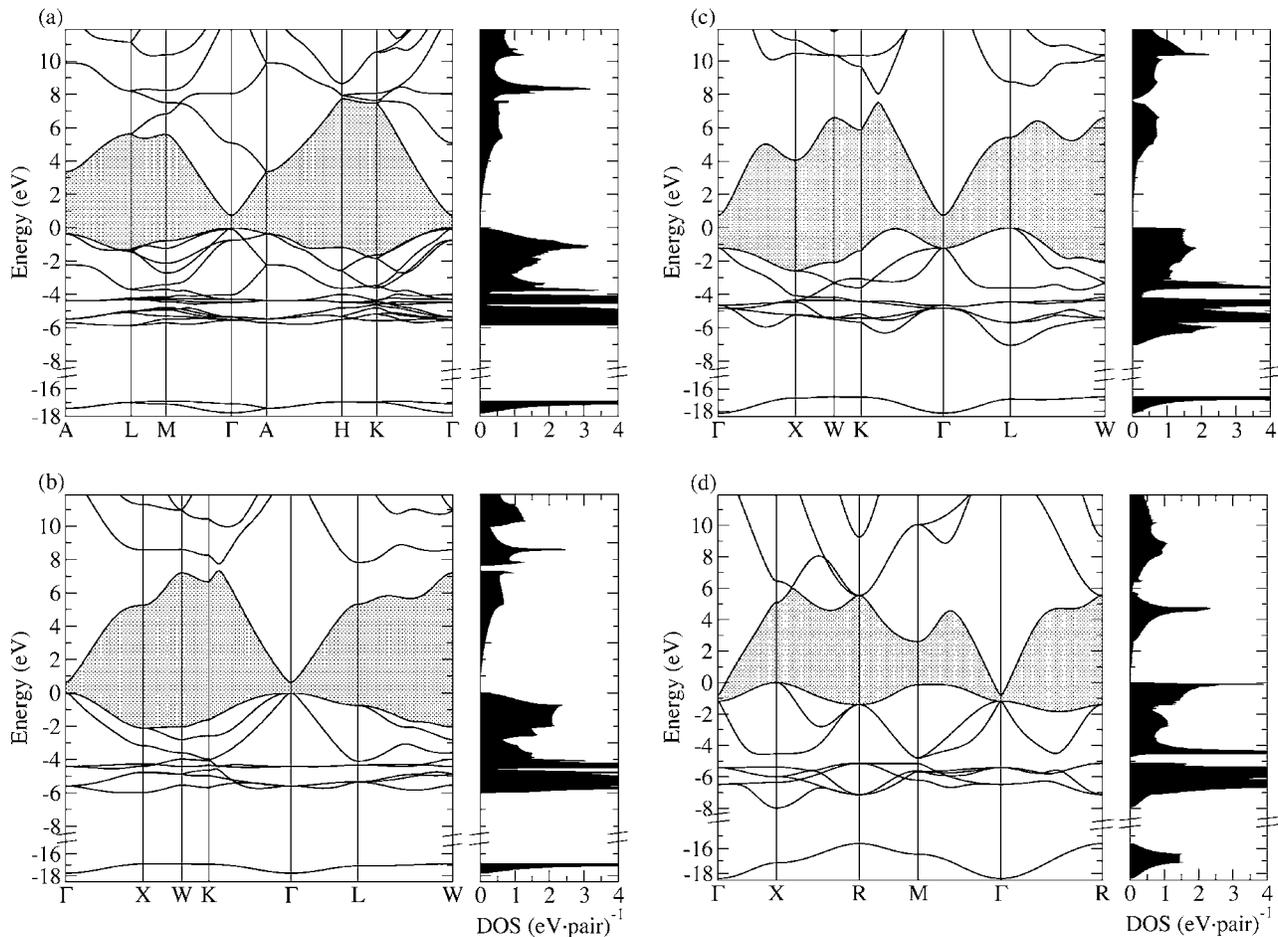
FIG. 5. Band structure and density of states (normalized per pair) for ZnO polymorphs calculated within the DFT-GGA framework: (a) wurtzite, (b) zinc blende, (c) rocksalt, and (d) cesium chloride. The shaded region indicates the fundamental gap. The valence band maximum is chosen as energy zero.

the pd repulsion is larger but does not give rise to a negative $\Gamma_1(s)-\Gamma_{15}(pd)$ gap as found there.[57]

Using QP corrections the small energy gaps obtained within DFT-GGA are significantly opened. With appropriate parameters as bond polarizability 0.78, nearest-neighbor distance 2.01 Å, and electronic dielectric constant 4.0[58] for the tetrahedrally coordinated ZnO the Bechstedt–Del Sole formula gives a QP shift of about 1.95 eV. This gap correction is bracketed by other approximate values of 0.85 eV,[59] 1.04 eV,[60] and 2.49 eV.[61] However, it agrees well with the value 1.67 eV derived within a sophisticated QP calculation.[47] Our values resulting for the direct fundamental gap at Γ 2.6 eV (w) or 2.59 eV (zb) are larger than the QP gap value of 2.44 eV[47] but still clearly underestimate the experimental gap of 3.44 eV.[62,63] This underestimation is sometimes related to the overscreening within the random-phase approximation (RPA) used in the QP approach.[47] We claim that one important reason is the overestimation of the pd repulsion and, hence, the too high position of the VBM in energy due to the too shallow d bands in LDA/GGA. Even when including many-body effects, the Zn3d bands are still to high in energy. For a better treatment of the QP effects also for the semicore d states, the pd repulsion should be reduced, which requires the inclusion of nondiagonal ele-

ments of the self-energy operator or the use of a starting point different from LDA/GGA, e.g., a generalized KS scheme.[64] A recent work[55] reported that rocksalt ZnO has an indirect band gap of 2.45±0.15 eV measured from optical absorption. Using the above-estimated QP shift of 1.95 eV and the indirect gap in DFT-LDA quality of 0.75 eV one finds a QP value of 2.60 eV close to the measured absorption edge.

In the case of the same polymorph the band structure and density of states of CdO in Fig. 6 show several similarities with those for ZnO. At about 15.5–17 eV below the VBM occur the $O2s$ bands, and the Cd4d bands are observed in the energy interval from −5.9 to −6.6 eV. The uppermost $O2p$-derived valence bands possess a maximum band width of about 3.3 eV, a value smaller than that found in recent photoemission studies.[65] Usually the conduction bands are well separated from the valence bands. However, for all polymorphs the lowest conduction band shows a pronounced minimum at the center of the BZ. Within an energy range of a few tenths of an electron volt above its bottom, this band is isotropic but highly nonparabolic.

In rs-CdO we find a direct gap of about 0.66 eV at the Γ point. As in the case of rs-ZnO also for rs-CdO the maxima of the valence bands occur at the L point and at the Σ line between Γ and K. These maxima lie above the CBM, which
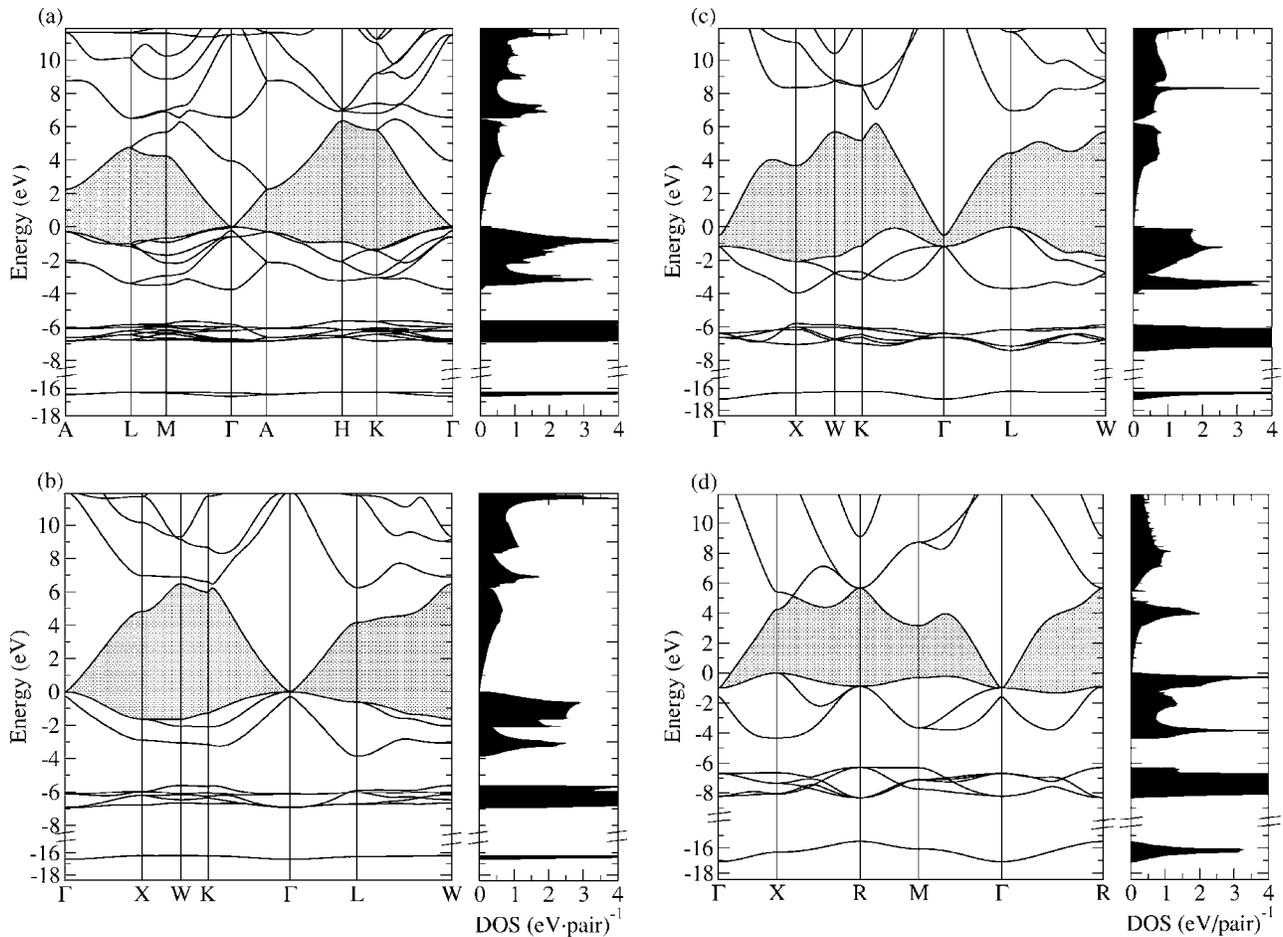
FIG. 6. Band structure and density of states (normalized per pair) for CdO polymorphs calculated within the DFT-GGA framework: (a) wurtzite, (b) zinc blende, (c) rocksalt, and (d) cesium chloride. The shaded region indicates the fundamental gap. The valence band maximum is chosen as energy zero.

results in negative indirect gaps of about −0.51 and −0.43 eV, and therefore our band structure indicates a half-metal. As described for rs-ZnO, the pd repulsion is responsible for this effect.[66] Our band structure is in qualitative agreement with a DFT-LDA calculation,[65] in particular with respect to the band dispersions. However, Ref. 65 found positive direct and indirect gap values. The gap opening of about 1 eV with respect to our values may be a consequence of the used basis set restricted to a few Gaussians. Corresponding experimental values are 0.84 and 1.09 eV for the indirect gaps and 2.28 eV for the lowest direct gap at Γ. Their comparison with the values calculated within DFT-GGA indicates effective QP gap openings of about 1.3–1.7 eV. However, these values should be considerably influenced by the pd repulsion, at least outside the BZ center. While the Cd4d bands are about 6.4 or 6.6 eV below the valence band maximum at Γ, the experimental distances are about 12.4 or 13.3 eV (with respect to the Fermi level).[67] A more recent measurement indicates an average binding energy of Cd4d relative to VBM of about 9.4 eV.[65] Altogether the band structures of CdO are rather similar to those of InN.[68] Within DFT-GGA in both cases small negative s-p fundamental gaps are found near Γ. The main difference is related with the position of the 4d bands, because the binding energy of In4d electrons is larger than that of Cd4d electrons.

The band structures presented in Figs. 4, 5, and 6 show clear chemical trends along the series MgO, ZnO, and CdO for a fixed crystal structure. To clarify these trends we list in Table III some energy positions for the two most important polymorphs—rocksalt and wurtzite. Among these energies we also list the lowest conduction and highest valence bands for two high-symmetry points in the corresponding fcc (Γ, L) or hexagonal (Γ, A) BZ. In the case of the cubic systems the position of the twofold (threefold) degenerate shallow core d level Γ_{12} $(\Gamma_{25'})$ at Γ is given. For the rocksalt phase as well as the wurtzite polymorph the level positions follow a clear chemical trend with the cations Mg, Zn, and Cd. The energetical position of the empty conduction-band levels as well as the filled valence-band states decreases with respect to the VBM. Consequently, the average gaps decrease along the series MgO, ZnO, and CdO. At least for tetrahedrally coordinated compounds the general trend is governed by both the splitting of the s- and p-valence energies as well as the nearest-neighbor distances.[58] In the case of wurtzite the effect of the nonmonotonous behavior of both quantities may give a monotonous net effect. Another atomic tendency, the increasing cation-p–anion-d splitting from ZnO to CdO,[56,58]

TABLE III. Characteristic energy levels (in eV) in the band structure of the rocksalt and wurtzite polymorphs of MgO, ZnO, and CdO as calculated within the DFT-GGA framework. The center Γ of the BZ and an L and A point at the BZ surface in [111]/[0001] direction are chosen for the Bloch wave vectors. The lowest conduction (c) bands and the highest valence (v) bands are studied. In the case of rocksalt also the positions of the Γ_{12} and $\Gamma_{25'}$ d bands are given. The uppermost Γ_{15v} or Γ_{6v} valence band at Γ is used as energy zero.

	Rocksalt				Wurtzite		
Level	MgO	ZnO	CdO	Level	MgO	ZnO	CdO
				Γ_{3c}	8.62	5.08	3.95
Γ_{1c}	4.50	1.97	0.66	Γ_{1c}	3.68	0.73	−0.20
Γ_{15v}	0.00	0.00	0.00	Γ_{6v}	0.00	0.00	0.00
				Γ_{1v}	0.31	−0.09	−0.07
Γ_{12}	⋯	−3.43	−5.22	Γ_{5v}	−0.30	−0.76	−0.60
$\Gamma_{25'}$	⋯	−3.61	−5.48	Γ_{3v}	−2.79	−4.03	−3.76
$L_{2'c}$	7.76	6.65	5.60	$A_{1,3c}$	6.11	3.36	2.26
L_{3v}	−0.62	1.22	1.17	$A_{5,6v}$	−0.15	−0.37	−0.27
L_{1v}	−4.48	−2.38	−2.52	A_{5v}	−1.61	−2.24	−2.12

is correlated with the increase of the distance of the d bands to the VBM.

We have also computed the volume deformation potentials for the direct gaps at Γ in rocksalt MgO to $a_V = -9.39$ eV and in wurtzite ZnO to $a_V = -1.55$ eV, as well as for the indirect gap between L and Γ in rocksalt CdO to $a_V = -1.87$ eV. The absolute value of the gap deformation potential of MgO is clearly larger than those of ZnO or CdO, due to the stronger bonding in MgO. Despite different gap states and ground-state polymorphs the values for ZnO and CdO are rather similar. Their smallness is a consequence of the large ionicity and the relatively large bond length. According to the estimate of Ref. 8, this may explain the small gaps of ZnO and CdO in comparison to ZnS and CdS. The deformation potential $a_V = -1.55$ eV calculated for w-ZnO within DFT-GGA is much smaller compared to the experimental value of $a_V = -3.51$ eV.[69] The reason should be the neglect of the large QP corrections not taken into account.

B. Dielectric functions and optical properties

For computing the dielectric function $\varepsilon(\omega)$ we have chosen the wurtzite and rocksalt polymorphs since they give the equilibrium geometries. In addition, we show spectra for zinc-blende crystals because of the mentioned similarity with wurtzite, but without its optical anisotropy. In Figs. 7–9 the influence of the crystallographic structure and of the anion on the dielectric function of a group-II oxide is demonstrated.

We observe that the change of the coordination of the atoms has a strong influence, which perhaps is best noticeable in the imaginary parts of the dielectric function. Going from the fourfold (w, zb) to the sixfold (rs) coordination, the absorption edge shifts toward higher photon energies and the oscillator strength increases. Thereby the screening sum rule is less influenced. One observes a clear increase of the (high-frequency) electronic dielectric constant $\varepsilon_\infty = \Re(\varepsilon(0))$ along the series MgO, ZnO, and CdO, so the main influence is due

to the chemistry. For the rs structure we compute $\varepsilon_\infty = 3.16$, 5.32, 7.20 in qualitative agreement with the reduction of the fundamental gap. Thereby, for CdO the accuracy is reduced due to the difficulties with the DFT-GGA band structure discussed above.

In the real parts there are several features that are similar, independent of the polymorph. There is only small variation of the ε_∞ with the different polymorphs. In the case of ZnO we find $\varepsilon_{\infty xx} = 5.24$, $\varepsilon_{\infty zz} = 5.26$ (w), $\varepsilon_\infty = 5.54$ (zb), and $\varepsilon_\infty = 5.32$ (rs). These values are larger than the constants $\varepsilon_{\infty xx} = 3.70$ and $\varepsilon_{\infty zz} = 3.75$ measured for w-ZnO.[7] This fact may be traced back to the underestimation of the fundamental gap within DFT-GGA. With the values $\varepsilon_\infty = 2.94$ (measured[7]) and $\varepsilon_\infty = 3.16$ (this work) the agreement is much better for rs-MgO.

The line shapes resulting from the dielectric function are discussed in detail for ZnO (Fig. 8). For smaller frequencies the curves $\Re(\varepsilon(\omega))$ exhibit maxima close to the absorption edge. These maxima are followed by regions with the general tendency for reduced intensity but modulated by peak structures related to critical points in the BZ. For frequencies larger than about 12.5 eV the real part becomes negative for all polymorphs. For the imaginary part in Fig. 8 the differences are larger—in agreement with the results of other calculations.[39] In the case of rocksalt there is a monotonous increase to the first main peaks at $\hbar\omega = 5.5$ and 7.0 eV which should be shifted toward higher energies in the experimental spectra according to the huge QP shifts discussed for the band structure. These two peaks are due to transitions near the L and X points of the fcc BZ (cf. Fig. 5). Therefore they can be classified as E_1 and E_2 transitions.[70] The subsequent peaks at about 9.5, 12.0, and 13.2 eV should be related to E_1' (i.e., second valence band into lowest conduction band at L) and E_2' transitions. We find a different situation for the wurtzite and zinc-blende structures. One observes a steep onset of the absorption just for photon energies only slightly larger than the fundamental band gap. In a range of about 4 eV it follows a more or less constant or even concave region. Such
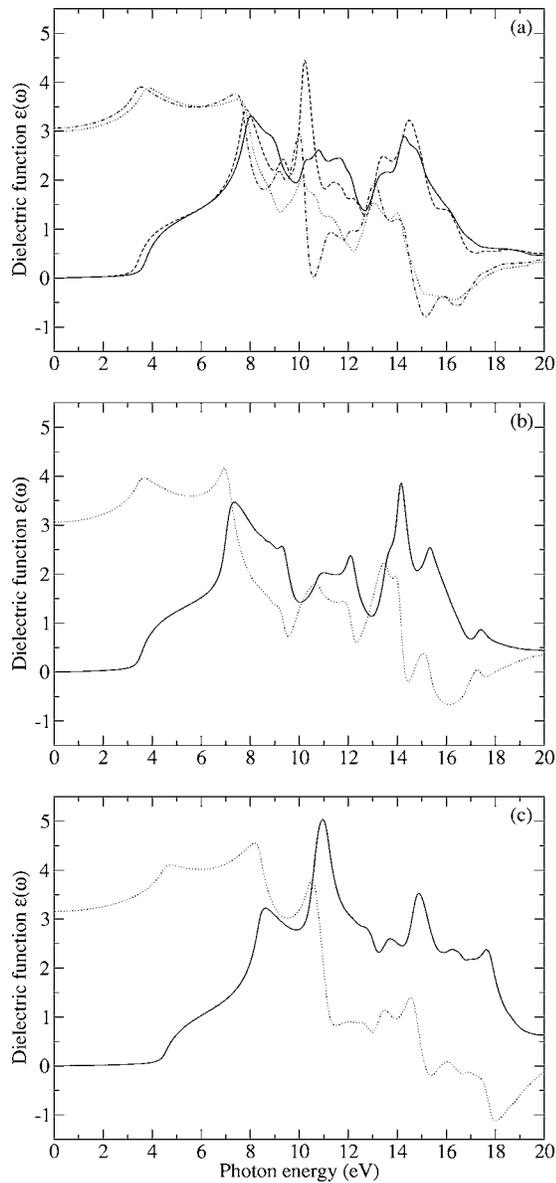
FIG. 7. Real and imaginary part of the frequency-dependent dielectric function for MgO polymorphs wurtzite (a), zinc blende (b), and rocksalt (c) as calculated within the independent-particle approximation using Kohn-Sham eigenstates and eigenvalues from DFT-GGA. Imaginary part: solid line, real part: dotted line. In the case of wurtzite besides the tensor components $\varepsilon_{xx}(\omega)=\varepsilon_{yy}(\omega)$ also the zz-component $\varepsilon_{zz}(\omega)$ is presented (imaginary part: dashed line, real part: dash-dotted line).

FIG. 8. Real and imaginary part of the frequency-dependent dielectric function for ZnO polymorphs wurtzite (a), zinc blende (b), and rocksalt (c) as calculated within the independent-particle approximation using Kohn-Sham eigenstates and eigenvalues from DFT-GGA. Imaginary part: solid line, real part: dotted line. In the case of wurtzite besides the tensor components $\varepsilon_{xx}(\omega)=\varepsilon_{yy}(\omega)$ also the zz-component $\varepsilon_{zz}(\omega)$ is presented (imaginary part: dashed line, real part: dash-dotted line).

a line shape is clearly a consequence of the pronounced conduction-band minimum near Γ, the nonparabolicity of the conduction band and the light-hole valence band. It has also been observed experimentally.[71] We therefore have a rather similar situation in the case of InN,[68] the III-V compound with constituents neighboring CdO in the periodic table of elements.

Within a four-band $\mathbf{k}\cdot\mathbf{p}$ Kane model one finds for the imaginary part of the dielectric function in the case of cubic systems[68]

$$\Im(\varepsilon(\omega))=\frac{1}{3}\left(\frac{e^2}{2a_BE_p}\right)^{1/2}\sqrt{1-x}\left[\sqrt{1+x}+8\right]\theta(1-x)\Big|_{x=E_g/\hbar\omega}$$

$$(1)$$

with the Bohr radius a_B, the fundamental direct band gap E_g, and the characteristic energy E_p, which is related to the square of the momentum-operator matrix element between s and p valence states. Indeed formula (1) leads to a constant $\Im(\varepsilon(\omega))=3(e^2/2a_BE_p)^{1/2}$ for $\hbar\omega\gg E_g$, i.e., away from the absorption edge. Interestingly the absolute plateau values in
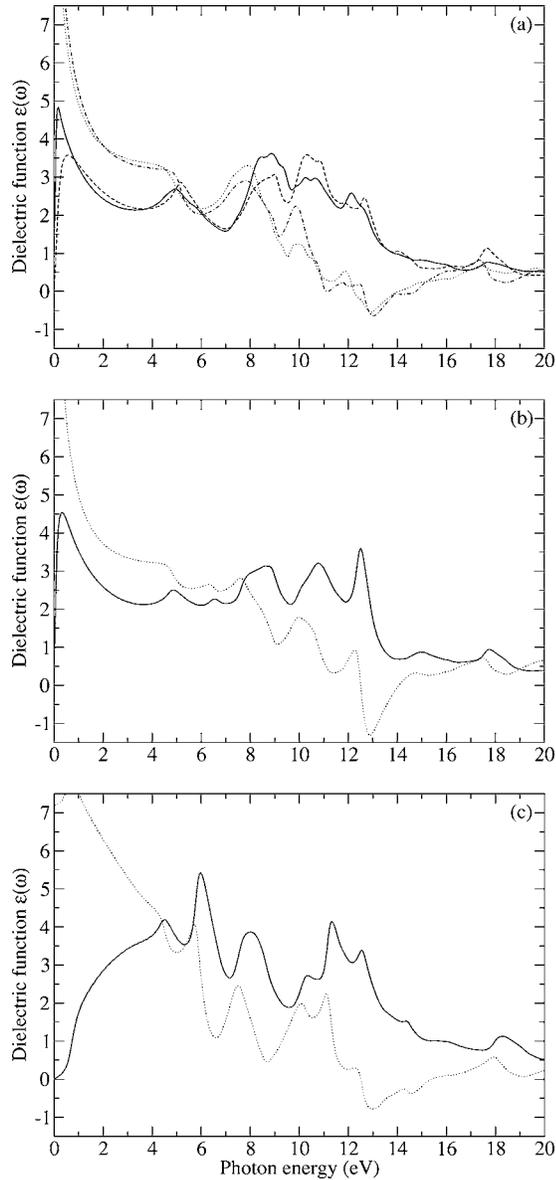
FIG. 9. Real and imaginary part of the frequency-dependent dielectric function for CdO polymorphs wurtzite (a), zinc blende (b), and rocksalt (c) as calculated within the independent-particle approximation using Kohn-Sham eigenstates and eigenvalues from DFT-GGA. Imaginary part: solid line, real part: dotted line. In the case of wurtzite besides the tensor components $\varepsilon_{xx}(\omega)=\varepsilon_{yy}(\omega)$ also the zz-component $\varepsilon_{zz}(\omega)$ is presented (imaginary part: dashed line, real part: dash-dotted line).

Figs. 8(a) and 8(b) of about 1.8 may be related to an energy E_p of about ≈ 37 eV, a value which is not too far from those in other estimations.[72,73] The same $\mathbf{k}\cdot\mathbf{p}$ model gives for the conduction-band mass near Γ the expression $m^{*}=m_0/[1+E_p/E_g]$. With an experimental gap energy of $E_g \approx 3.4$ eV it results an electron mass of about $m^{*}=0.09m_0$ somewhat smaller than the experimental value of about $0.19m_0$ (Ref. 73) or $0.28m_0$.[7] From the conduction band minima plotted in Figs. 5(a) and 5(b) we derive band masses in DFT-GGA quality of about $m^{*}=0.153m_0$ (zb) and $m^{*}=0.151m_0/0.150m_0$ (w) with a negligible anisotropy. Ab-

sorption peaks occur at higher photon energies at about 7.5, 9.1, and 10.6 eV for zb-ZnO and 6.5, 9.9, and 10.7 eV for w-ZnO. These peaks may be related to E_1/E_2, E_1', and E_2' transitions in the case of the zinc-blende structure. For the wurtzite polymorph the interpretation is more difficult, however, the lowest peak should mainly be caused by transitions on the LM line between the highest valence band and the lowest conduction band.

We have to mention that the influence of many-body effects such as QP shifts[44–46] and excitonic effects[74] has been neglected. The QP effects lead to a noticeable blueshift of the absorption spectra, while the excitonic effects, basically the electron-hole pair attraction, give rise to a redshift and a more or less strong mixing of interband transitions. Furthermore, the neglected effects should cause a redistribution of spectral strength from higher to lower photon energies.[68]

V. SUMMARY AND CONCLUSIONS

Using the *ab initio* density functional theory together with a generalized gradient corrected exchange-correlation functional, we have calculated the ground-state and excited-state properties of several polymorphs of the group-II oxides MgO, ZnO, and CdO. We have especially studied the rocksalt and wurtzite structures which give rise to the equilibrium geometries of the oxides. Zinc blende has been investigated to study the same local tetrahedron bonding geometry but without the resulting macroscopic anisotropy. Cesium chloride is an important high-pressure polymorph. In addition, two hexagonal structures, nickel arsenide and h-MgO, have been studied for MgO.

In agreement with experimental and other theoretical findings the rocksalt (wurtzite) structure has been identified as the equilibrium geometry of MgO and CdO (ZnO). The non-isostructural series of the three compounds with a common anion has been related to the nonmonotonous variation of the cation size along the column Mg, Zn, and Cd. We calculated binding energies which are in good agreement with measured values. MgO and CdO undergo a pressure-induced phase transition from the NaCl into the CsCl structure. w-ZnO first transforms into rocksalt geometry but also shows a phase transition into the cesium chloride geometry at higher hydrostatic pressures. Our values for the transition pressures agree well with predictions of other *ab initio* calculations and experimental observations. We predicted the possibility of pseudomorphic growth of MgO in biaxially strained wurtzite geometry on a w-ZnO substrate.

The atomic coordination and hence the polymorph has a strong influence on the distribution of the allowed Bloch energies. This fact has been clearly demonstrated by the comparison of band structures and densities of states computed for different crystallographic structures. This fact holds in particular for the fundamental energy gaps which however strongly suffer from the neglect of the excitation aspect, the so-called QP corrections. In the case of ZnO and CdO the semicore Zn3d and Cd4d states also contribute to the gap shrinkage. In the framework of DFT-GGA they are too shallow and hence give rise to an overestimation of the pd repulsion (which shifts the uppermost p-like valence band to-

wards higher energies). The effect of the crystal structure on the dielectric function is weaker as in the case of the band structures due to the occurring Brillouin-zone integration. We found a stronger influence of the cation. A clear chemical trend has been observed for the electronic dielectric constants. Along the series MgO, ZnO, and CdO also the averaged spectral strength increases. The crystal structure has the most influence on the line shape of the absorption edge. This effect has been intensively discussed for ZnO. For the wurtzite and zinc-blende polymorphs we observe a steep onset in

the absorption, followed by a plateau-like frequency region.

[1] M. Joseph, H. Tabata, and T. Kawai, Jpn. J. Appl. Phys., Part 1 **38**, L1205 (1999).
[2] M. Venkatesan, C. B. Fitzgerald, J. G. Lunney, and J. M. D. Coey, Phys. Rev. Lett. **93**, 177206 (2004).
[3] C. Klingshirn, H. Priller, M. Decker, J. Brückner, H. Kalt, R. Hauschild, J. Zeller, A. Waag, A. Bakin, H. Wehmann, K. Thonke, R. Sauer, R. Kling, F. Reuss, and Ch. Kirchner, Adv. Solid State Phys. **45**, 275 (2005).
[4] Ü. Özgür, Ya. I. Alivov, C. Liu, A. Teke, M. A. Reshchikov, S. Doğan, V. Avrutin, S.-J. Cho, and H. Morkoç, J. Appl. Phys. **98**, 041301 (2005).
[5] Landolt-Börnstein, *Numerical Data and Functional Relationships*, Semiconductors: Physics of II-VI and I-VII Compounds, Semimagnetic Semiconductors Science and Technology Vol. 17, Part b, edited by O. Madelung (Springer, Berlin, 1984).
[6] D. M. Roessler and W. C. Walker, Phys. Rev. **159**, 733 (1967).
[7] *Springer Handbook of Condensed Matter and Materials Data*, edited by W. Martienssen and H. Warlimont (Springer, Berlin, 2005).
[8] P. Carrier and S.-H. Wei, J. Appl. Phys. **97**, 033707 (2005).
[9] P. Hohenberg and W. Kohn, Phys. Rev. **136**, B864 (1964).
[10] W. Kohn and L. J. Sham, Phys. Rev. **140**, A1133 (1965).
[11] J. P. Perdew, in *Electronic Structure of Solids '91*, edited by P. Ziesche and H. Eschrig (Akademie, Berlin, 1991), p. 11.
[12] G. Kresse and D. Joubert, Phys. Rev. B **59**, 1758 (1999).
[13] B. Adolph, J. Furthmüller, and F. Bechstedt, Phys. Rev. B **63**, 125108 (2001).
[14] P. E. Blöchl, Phys. Rev. B **50**, 17953 (1994).
[15] G. Kresse and J. Furthmüller, Comput. Mater. Sci. **6**, 15 (1996); Phys. Rev. B **54**, 11169 (1996).
[16] H. J. Monkhorst and J. D. Pack, Phys. Rev. B **13**, 5188 (1976).
[17] P. E. Blöchl, O. Jepsen, and O. K. Andersen, Phys. Rev. B **49**, 16223 (1994).
[18] H. Ehrenreich and M. H. Cohen, Phys. Rev. **115**, 786 (1959).
[19] http://cst-www.nrl.navy.mil/lattice/struk/b_k.html
[20] S. Limpijumnong and W. R. L. Lambrecht, Phys. Rev. B **63**, 104103 (2001).
[21] G. Cappellini, V. Fiorentini, K. Tenelsen, and F. Bechstedt, Mater. Res. Soc. Symp. Proc. **395**, 429 (1996).
[22] F. D. Murnaghan, Proc. Natl. Acad. Sci. U.S.A. **30**, 244 (1944).
[23] *Handbook of Chemistry and Physics*, 79th ed., edited by D. R. Lide (CRC, Boca Raton, FL, 1998).
[24] Landolt-Börnstein, *Numerical Data and Functional Relationships*, Crystal Structure Data of Inorganic Compounds Vol. 7, Part b (Springer, Berlin, 1975).
[25] J. E. Jaffe, J. A. Snyder, Z. Lin, and A. C. Hess, Phys. Rev. B **62**, 1660 (2000).
[26] B. B. Karki, R. M. Wentzcovitch, S. de Gironcoli, and S. Baroni, Phys. Rev. B **61**, 8793 (2000).
[27] A. R. Oganov and P. I. Dorogokupets, Phys. Rev. B **67**, 224110 (2003).
[28] F. Decremps, F. Datchi, A. M. Saitta, A. Polian, S. Pascarelli, A. DiCicco, J. P. Itié, and F. Baudelet, Phys. Rev. B **68**, 104101 (2003).
[29] H. Karzel, W. Potzel, M. Köfferlein, W. Schiessl, M. Steiner, U. Hiller, G. M. Kalvius, D. W. Mitchell, T. P. Das, P. Blaha, K. Schwarz, and M. P. Pasternak, Phys. Rev. B **53**, 11425 (1996).
[30] J. Serrano, A. H. Romero, F. J. Manjón, R. Lauck, M. Cardona, and A. Rubio, Phys. Rev. B **69**, 094306 (2004).
[31] S. Limpijumnong and S. Jungthawan, Phys. Rev. B **70**, 054104 (2004).
[32] J. M. Recio, M. A. Blanco, V. Luaña, R. Pandey, L. Gerward, and J. S. Olsen, Phys. Rev. B **58**, 8949 (1998).
[33] S. Desgreniers, Phys. Rev. B **58**, 14102 (1998).
[34] R. J. Guerrero-Moreno and N. Takeuchi, Phys. Rev. B **66**, 205205 (2002).
[35] J. Zhang, Phys. Chem. Miner. **26**, 644 (1999).
[36] *Table of Periodic Properties of Elements* (Sargent-Welch, Skokie, Illinois, 1980).
[37] A. Zunger, Phys. Rev. B **22**, 5839 (1980).
[38] J. M. Recio, M. A. Blanco, V. Luaña, R. Pandey, L. Gerward, and J. S. Olsen, Phys. Rev. B **58**, 8949 (1998).
[39] J. Sun, H.-T. Wang, J. He, and Y. Tian, Phys. Rev. B **71**, 125132 (2005).
[40] H. Liu, H. K. Mao, M. Somayazulu, Y. Ding, Y. Meng, and D. Häusermann, Phys. Rev. B **70**, 094114 (2004).
[41] K. Karch, F. Bechstedt, P. Pavone, and D. Strauch, Phys. Rev. B **53**, 13400 (1996).
[42] C. H. Bates, W. B. White, and R. Roy, Science **137**, 993 (1962).
[43] S. Limpijumnong and W. R. L. Lambrecht, Phys. Rev. Lett. **86**, 91 (2001).
[44] M. S. Hybertsen and S. G. Louie, Phys. Rev. B **34**, 5390 (1986).
[45] F. Bechstedt, Adv. Solid State Phys. **32**, 161 (1992).
[46] W. G. Aulbur, L. Jönsson, and J. W. Wilkins, Solid State Phys. **54**, 1 (2000).
[47] M. Usuda, N. Hamada, T. Kotani, and M. van Schilfgaarde, Phys. Rev. B **66**, 125101 (2002).
[48] G. Cappellini, S. Bouette-Russo, B. Amadon, C. Noguera, and F. Finocchi, J. Phys.: Condens. Matter **12**, 3671 (2000).
[49] B. Adolph, V. I. Gavrilenko, K. Tenelsen, F. Bechstedt, and R. Del

Sole, Phys. Rev. B **53**, 9797 (1996).

[50] U. Schönberger and F. Aryasetiawan, Phys. Rev. B **52**, 8788 (1995).

[51] E. L. Shirley, Phys. Rev. B **58**, 9579 (1998).

[52] F. Bechstedt and R. Del Sole, Phys. Rev. B **38**, 7710 (1988).

[53] R. C. Whited, C. J. Flaten, and W. C. Walker, Solid State Commun. **13**, 1903 (1973).

[54] N. P. Wang, M. Rohlfing, R. Krüger, and J. Pollmann, Appl. Phys. A: Mater. Sci. Process. **78**, 213 (2004).

[55] A. Segura, F. J. Manjón, A. Muñoz, and M. J. Herrera-Cabrera, Appl. Phys. Lett. **83**, 278 (2003).

[56] S. H. Wei and A. Zunger, Phys. Rev. B **37**, 8958 (1988).

[57] F. Bechstedt and J. Furthmüller, J. Cryst. Growth **246**, 315 (2002).

[58] W. A. Harrison, *Electronic Structure and the Properties of Solids* (Dover, New York, 1989).

[59] P. Rinke, A. Qteish, J. Neugebauer, C. Freysoldt, and M. Scheffler, New J. Phys. **7**, 126 (2005).

[60] H. Q. Ni, Y. F. Lu, and Z. M. Ren, J. Appl. Phys. **91**, 1339 (2002).

[61] M. Oshikiri and F. Aryasetiawan, Phys. Rev. B **60**, 10754 (1999).

[62] Y. S. Park, C. W. Litton, T. C. Collins, and D. C. Reynolds, Phys. Rev. **143**, 512 (1966).

[63] M. Oshikiri and F. Aryasetiawan, J. Phys. Soc. Jpn. **69**, 2123 (2000).

[64] F. Fuchs, J. Furthmüller, F. Bechstedt, M. Shishkin, and G. Kresse, arXiv:cond-mat/0604447 (2006).

[65] Y. Dou, R. G. Egdell, D. S. Law, N. M. Harrison, and B. G. Searle, J. Phys.: Condens. Matter **10**, 8447 (1998).

[66] J. E. Jaffe, R. Pandey, and A. B. Kunz, Phys. Rev. B **43**, 14030 (1990).

[67] C. J. Vesely and D. W. Langer, Phys. Rev. B **4**, 451 (1971).

[68] J. Furthmüller, P. H. Hahn, F. Fuchs, and F. Bechstedt, Phys. Rev. B **72**, 205106 (2005).

[69] A. Mang, K. Reimann, and St. Rübenacke, Solid State Commun. **94**, 251 (1995).

[70] P. Y. Yu and M. Cardona, *Fundamentals of Semiconductors* (Springer, Berlin, 1996).

[71] J. F. Muth, R. M. Kolbas, A. K. Sharma, S. Oktyabrsky, and S. Naryan, J. Appl. Phys. **85**, 7884 (1999).

[72] P. Lawaetz, Phys. Rev. B **4**, 3460 (1971).

[73] W. A. Harrison, *Elementary Electronic Structure* (World Scientific, Singapore, 1999).

[74] W. G. Schmidt, S. Glutsch, P. H. Hahn, and F. Bechstedt, Phys. Rev. B **67**, 085307 (2003).